This is a repository copy of *Dramatic Influence of A-Site Nonstoichiometry on the Electrical Conductivity and Conduction Mechanisms in the Perovskite Oxide Na0.5Bi0.5TiO3*.

White Rose Research Online URL for this paper:
http://eprints.whiterose.ac.uk/95564/

Version: Accepted Version

# The dramatic influence of A-site non-stoichiometry on the electrical conductivity and conduction mechanisms in the perovskite oxide $Na_{0.5}Bi_{0.5}TiO_3$

Ming Li[1], Huairuo Zhang[1], Stuart N. Cook[2], Linhao Li[1], John A. Kilner[2,3], Ian M. Reaney[1] and Derek C. Sinclair[1*]

[1]Department of Materials Science and Engineering, University of Sheffield, Sir Robert Hadfield Building, Mappin Street, Sheffield, S1 3JD, United Kingdom

[2]Department of Materials, Imperial College London, London, SW7 2AZ, United Kingdom

[3]International Institute for Carbon-Neutral Energy Research (I2CNER), 744 Motooka Nishi-ku Fukuoka 819-0395, Japan

* Author to whom correspondence should be addressed.

E-mail: d.c.sinclair@sheffield.ac.uk.

**Abstract**

Recently, there has been considerable interest in the perovskite phase $Na_{0.5}Bi_{0.5}TiO_3$ (NBT) as a promising lead-free piezoelectric material. Here we report low levels of Na nonstoichiometry ($\pm 2$ atom % on the A-site) in the nominal starting composition of NBT ceramics can lead to dramatic changes in the magnitude of the bulk (grain) conductivity ($\sigma_b$) and the conduction mechanism(s). Nominal starting compositions with Na-excess exhibit high levels of oxide-ion conduction with $\sigma_b \sim 2.2$ $mScm^{-1}$ (at 600 °C) and an activation energy ($E_a$) < 1 eV whereas those with Na-deficiency are dielectrics based on intrinsic electronic conduction across the band gap with $\sigma_b \sim 1.6$ $\mu Scm^{-1}$ (at 600 °C) and $E_a \sim 1.7$ eV. Drying of reagents especially $Na_2CO_3$ changes the starting stoichiometry slightly due to small amount of adsorbed moisture in the raw materials but influences significantly the electrical properties. This demonstrates the bulk electrical properties of NBT to be highly sensitive to low levels of A-site nonstoichiometry and reveals how to fine-tune the nominal starting composition of NBT ceramics to suppress leakage conductivity for piezoelectric and high temperature capacitor applications.

# 1. Introduction

Lead zirconate titanate ($Pb(Zr_{1-x}Ti_x)O_3$, PZT) has been the most widely used piezoelectric material in applications of actuators, sensors and transducers since the 1950s. The toxicity of lead has raised environmental concerns for many years and consequently has led to extensive studies on developing lead-free piezoelectric materials over the past decade.[1-4] The perovskite oxide $Na_{0.5}Bi_{0.5}TiO_3$ (NBT) is one of the favoured candidates to replace PZT and various solid solutions with other ferroelectric materials such as $BaTiO_3$ and $K_{1-x}Na_xNbO_3$ have been studied both for piezoelectric and high temperature capacitor (dielectric) applications.[5-17]

NBT has a complex crystal structure.[18-25] Early neutron powder diffraction studies proposed NBT to exhibit a rhombohedral (space group R3c) structure at room temperature (RT).[18] Recent high resolution synchrotron powder x-ray diffraction data suggest a monoclinic structure with space group Cc is a better fit.[19] Furthermore, the average structure determined by neutron powder diffraction and synchrotron powder x-ray diffraction is different from the local structure, as revealed by X-ray and neutron total scattering experiments and pair distribution function (PDF) analysis.[20,21] The local deviations from the average structure occur because of distinctly different displacements of Na and Bi ions[20] and complex in-phase and out-of-phase octahedral tilting.[22] The complexity of the local structure has been directly demonstrated by transmission electron microscopy,[22] which confirms an essentially random distribution of Bi and Na and reveals significant disorder of the octahedral rotations and cation displacements. It has been proposed that NBT consists of nanoscale domains which exhibit $a^-a^-c^+$ in-phase tilting at a length limited to only a few unit cells. Assemblages of such nanodomains exhibit an average $a^-a^-c^-$ anti-phase tilting system and the authors of Ref. 22 refer to the structure as being best described by a 'continuous tilt' model. Such a model is

consistent with the 'average' monoclinic Cc symmetry from synchrotron powder x-ray diffraction data.[19]

Apart from its complex crystal structure, NBT also exhibits unexpected, interesting electrical and piezoelectric properties.[26-29] Small deviations in nominal A-site cation stoichiometry change the RT dc resistivity of NBT by three orders of magnitude and influence the piezoelectric and dielectric properties.[26] In particular, Na-excess (eg $Na_{0.51}Bi_{0.50}TiO_{3.005}$) or Bi-deficiency (eg $Na_{0.50}Bi_{0.49}TiO_{2.985}$) in the starting composition lowers dc resistivity and the piezoelectric coefficient ($d_{33}$) but enhances the depolarization temperature ($T_d$). In contrast, Na-deficiency (eg $Na_{0.49}Bi_{0.50}TiO_{2.995}$) or Bi-excess (eg $Na_{0.50}Bi_{0.51}TiO_{3.015}$) in the starting composition enhances the dc resistivity and $d_{33}$ but lowers $T_d$.[26-28] Of particular interest is the origin of the change in NBT resistivity by small variations in the nominal starting Na and Bi concentrations.

In a previous study,[30] we used a combination of Impedance Spectroscopy, $^{18}O$ tracer diffusion studies and transport number measurements for oxide-ion conductivity to reveal the effect of Bi nonstoichiometry on the electrical properties of $Na_{0.50}Bi_{0.50+x}TiO_{3+1.50x/2}$ where x = -0.01 ($Na_{0.50}Bi_{0.49}TiO_{2.985}$; $NBi_{0.49}T$), 0 ($Na_{0.50}Bi_{0.50}TiO_3$; NBT) and 0.01 ($Na_{0.50}Bi_{0.51}TiO_{3.015}$; $NBi_{0.51}T$). The defect chemistry of NBT is rather different from other well-known titanates such as $(Ba,Sr,Ca)TiO_3$ in that the electrical conductivity is dominated by oxide-ion conduction in NBT and $NB_{0.49}T$ rather than electronic conduction. We have attributed the differences in behaviour and the high oxide-ion conductivity in these compositions to high oxygen ion mobility associated with highly polarised $Bi^{3+}$ cations and weak Bi-O bonds[31] as well as oxygen vacancies generated through loss of a small amount of $Bi_2O_3$ during ceramic processing according to the Kroger-Vink equation,

$$2Bi_{Bi}^{\times} + 3O_O^{\times} \rightarrow 2V_{Bi}''' + 3V_O^{\bullet\bullet} + Bi_2O_3 \qquad (1)$$
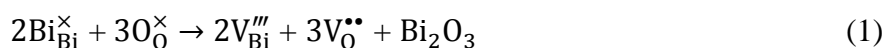
In contrast, excess $Bi_2O_3$ in $NB_{0.51}T$ can compensate for the loss obtained during sample processing, therefore creating a final composition in sintered ceramics that is close to stoichiometric NBT. Thus, the oxide-ion conductivity is suppressed and $NB_{0.51}T$ exhibits intrinsic electronic conduction.

Interestingly, Na nonstoichiometry in the starting composition also influences the electrical and piezoelectric properties of NBT but in a different way compared to Bi nonstoichiometry.[26,27] Na-excess starting compositions exhibit higher RT dc conductivity than those that are Na-deficient. Based on equation (1), this appears somewhat counter intuitive. Excess $Na_2O$ in the starting composition should help to compensate for the bismuth and oxygen deficiency induced by $Bi_2O_3$-loss during ceramic processing. This should suppress the oxide-ion conductivity, whereas Na-deficiency may be expected to increase the A-site deficiency and oxygen vacancy concentration and therefore increase the oxide-ion conductivity. This raises an interesting question regarding the nature of the A-site nonstoichiometry in NBT and how to control the nominal starting composition to optimise its piezoelectric and dielectric properties.

Here we report on the defect chemistry of nominal Na nonstoichiometric NBT compositions, $Na_{0.50+y}Bi_{0.50}TiO_{3+0.50y}$ (y= 0.01 and -0.01, named as $Na_{0.51}BT$ and $Na_{0.49}BT$, respectively) and clarify the origin(s) of its effect on electrical properties. We also highlight the importance of drying $Na_2CO_3$ prior to ceramic processing as small changes in the nominal starting stoichiometry of this hygroscopic reagent influences the electrical properties of NBT ceramics.

## 2. Experimental Section

Polycrystalline samples of $Na_{0.49}BT$, NBT and $Na_{0.51}BT$ were prepared using the conventional solid state route. $Na_2CO_3$ (99.5%, Sigma-Aldrich), $Bi_2O_3$ (99.9%, Acros

Organics) and $TiO_2$ (99.9%, Sigma-Aldrich) were used as raw materials. Prior to weighing, $Na_2CO_3$, $Bi_2O_3$ and $TiO_2$ were dried (unless stated otherwise) at 300, 180 and 800 °C for 8 h, respectively. Mixtures of raw materials were ball milled using $Y_2O_3$-stabilised $ZrO_2$ grinding media for 6 h, dried, sieved and calcined at 800 °C for 2 h. The resultant powders were ball milled for 4 h followed by a second calcination at 850 °C for 2 h and ball milled for 6 h. Pellets were sintered at 1125-1150 °C for 2 h in air and covered using powders of the same composition during sintering.

The moisture content in raw materials was examined using a PerkinElmer Pyris 1 and a Setaram SETSYS Evolution thermo-gravimetric analysis (TGA). A combination of X-ray diffraction (XRD), scanning electron microscopy (SEM), scanning transmission electron microscopy (STEM) and energy dispersive x-ray spectroscopy (EDS) were employed to examine the phase purity and ceramic microstructure. Impedance Spectroscopy measurements were performed using an Agilent E4980A, an HP 4192A impedance analyser and a Solartron 1260 system. Au or Pt paste electrodes were used. IS data were corrected for sample geometry (thickness/area of pellet). High frequency instrumental-related (impedance analyser, lead, and sample jig) inductance effects were corrected by performing a short circuit measurement.

For $^{18}O$ tracer diffusion measurements, the standard procedure for introducing an $^{18}O$ penetration profile into a solid from a large volume of gas was employed.[32,33] Dense samples (relative density > 95%) were annealed in highly enriched $^{18}O_2$ gas. The oxygen isotope profiles were measured by means of time-of-flight secondary ion mass spectrometry (ToF-SIMS, ION-TOF GmbH, Münster, Germany). More detailed experimental information can be found in Supplementary Information in Ref. 30.

## 3. Results

**Phase purity and compositional analysis.** XRD patterns of $Na_{0.49}BT$, NBT and $Na_{0.51}BT$ after double calcination at 800 and 850 °C for 2 h showed no evidence of any secondary phase(s), Figure S1. The cell volume extracted using space group R3c with data collected using Si as an internal standard is similar for all three samples: 351.48 (14) $Å^3$ ($Na_{0.49}BT$); 351.49(9) $Å^3$ (NBT) and V=351.72 (10) $Å^3$ ($Na_{0.51}BT$). In contrast, SEM and EDS revealed a Na-rich secondary phase in $Na_{0.51}BT$, Figure S2d and STEM high angle annular dark field (HAADF) Z-contrast images revealed a small amount of $TiO_2$ secondary phase in $Na_{0.49}BT$, Figure S2e. The analysed main phase compositions of $Na_{0.49}BT$, NBT and $Na_{0.51}BT$ by EDS, Table S1, were close to the cation ratios in NBT and were not unambiguously distinguishable from each other within instrument resolution and standard errors. These results demonstrate the A-site non-stoichiometry to be very limited in NBT.

**Dielectric properties.** The small differences in starting composition have a modest influence on the magnitude and temperature of the relative permittivity maximum ($\varepsilon_{r,max}$ and $T_m$, respectively) but have a dramatic effect on the dielectric loss (tan $\delta$). The temperature dependence of $\varepsilon_r$, Figure 1a, reveals $Na_{0.51}BT$ to exhibit the highest $\varepsilon_{r,max}$ of ~3200 with $T_m$ ~315 °C. With decreasing Na-starting content, $\varepsilon_{r,max}$ decreases to ~3000 for NBT and ~2700 for $Na_{0.49}BT$; however, $T_m$ increases to ~320 °C for NBT and ~ 335 °C for $Na_{0.49}BT$. $Na_{0.51}BT$ and NBT exhibit high levels of dielectric loss (> 0.05) above ~ 300 °C, whereas $Na_{0.49}BT$ exhibits very low tan $\delta$ (< 0.005) in the range ~ 300 to 600 °C. The loss maximum observed at < 300 °C shifts to lower temperature with decreasing Na-starting content.
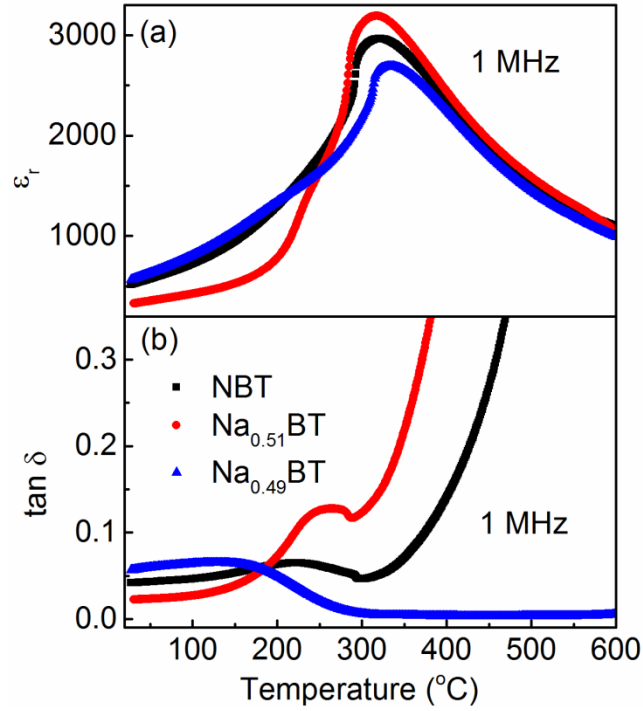
**Figure 1.** Temperature dependence of (a) $\varepsilon_r$ and (b) tan $\delta$ at 1 MHz for NBT, $Na_{0.51}BT$ and $Na_{0.49}BT$.

**Impedance Spectroscopy (IS).** Complex impedance plane, Z*, plots at 500 °C for the three samples are shown in Figure 2a-b. The single arc observed for $Na_{0.49}BT$ within the measured frequency range, Figure 2b, has an associated resistivity of ~ 9 MΩ cm, whereas the high frequency arc for NBT and $Na_{0.51}BT$, Figure 2a, has an associated resistivity of ~2 and 0.8 kΩ cm, respectively. The extracted $\varepsilon_r$ (~1600-1700) from the capacitance (C) associated with these arcs using the relationship $2\pi fRC=1$ at the arc maximum (where f is the frequency at the arc maximum) is consistent with the high bulk $\varepsilon_r$ value for this ferroelectric material (see Figure 1a), indicating these arcs are associated with the bulk (grain) response.

Bulk resistance ($R_b$) for the resistive and conducting samples exhibit different temperature dependence and therefore have different activation energy ($E_a$), as shown in the Arrhenius plot of the bulk conductivity ($\sigma_b$) where $\sigma_b = 1/R_b$, Figure 2c. The resistive sample $Na_{0.49}BT$ has a single slope with $E_a$ ~1.7 eV whereas for the two conducting samples NBT and

8

Na$_{0.51}$BT, there is a change in slope and therefore E$_a$ at T$_m$ associated with $\varepsilon_{r,max}$ (T$_m$ ~ 315-335 °C, Figure 1). E$_a$ is ~ 0.9 eV and 0.4-0.5 eV below and above T$_m$, respectively. The magnitudes of $\sigma_b$ and E$_a$ for Na$_{0.49}$BT and Na$_{0.51}$BT are very similar to that observed for NBi$_{0.51}$T and NBi$_{0.49}$T in our previous study of Bi-nonstoichiometry,[30] Figure 2c, respectively.

Further IS measurements to low frequency in different atmospheres revealed different conduction mechanisms in the resistive and conducting samples. For Na$_{0.51}$BT, the high frequency data associated with the bulk response remained unchanged on varying the atmospheres from O$_2$ to N$_2$, Figure 3a. The low frequency data showed a strong dependence on pO$_2$, Figure 3a-b. Capacitance associated with the distorted, low frequency arcs are in the range ~ 0.1 to 1 mF cm$^{-1}$. The independence of high frequency bulk data on pO$_2$ and the strong pO$_2$ dependence of the low frequency data together with the extremely high associated capacitance are consistent with Warburg diffusion and oxide-ion conduction in this sample.

The Z* plot at 600 °C for the resistive sample Na$_{0.49}$BT consists primarily of a large arc associated with the bulk response, Figure 3c. R$_b$ decreased from ~ 630 k$\Omega$ cm in air and O$_2$ to ~ 120 k$\Omega$ cm in N$_2$. There was no obvious change of R$_b$ in air and O$_2$, probably due to the small difference in pO$_2$ for these atmospheres. The dependence of R$_b$ on pO$_2$ suggests n-type electronic conduction to dominate in this sample. In addition, measurements down to 1 mHz revealed the Warburg diffusion arc to be heavily suppressed. Similar data were reported for the resistive NBi$_{0.51}$T sample in our previous study.[30]
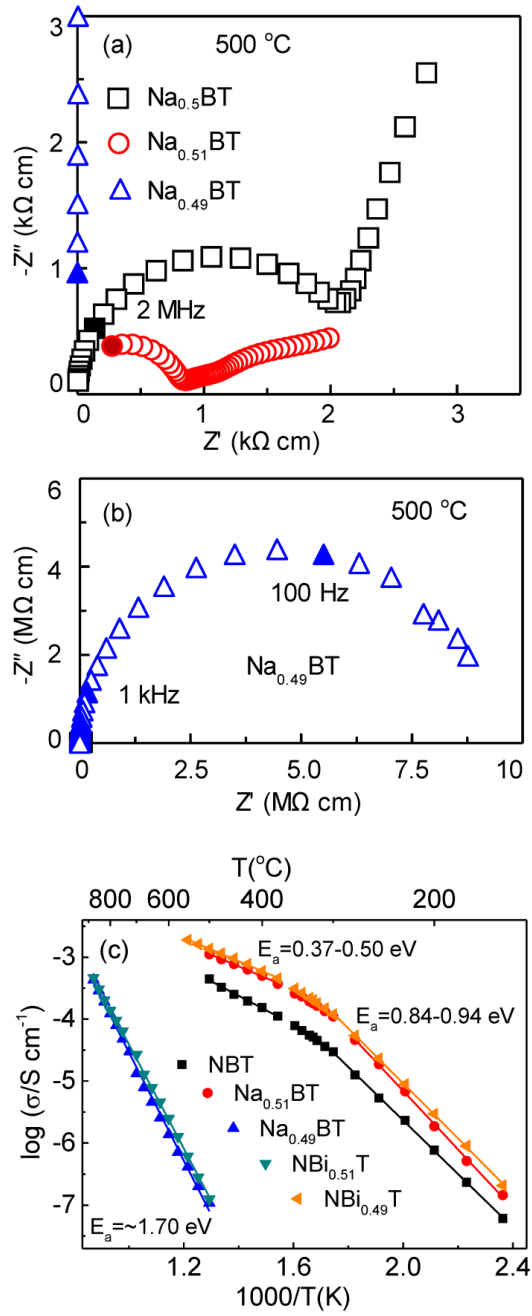
**Figure 2.** (a) Z* plots for NBT, $Na_{0.51}T$ and $Na_{0.49}T$ ceramics at 500 °C, (b) full scale view of data in (a) for $Na_{0.49}T$. Filled symbols indicate selected frequencies; (c) Arrhenius-type plots of bulk conductivity for all samples. For comparison, data for nonstoichiometric Bi-starting compositions $NBi_{0.51}T$ and $NBi_{0.49}T$ from Ref. 30 are provided.
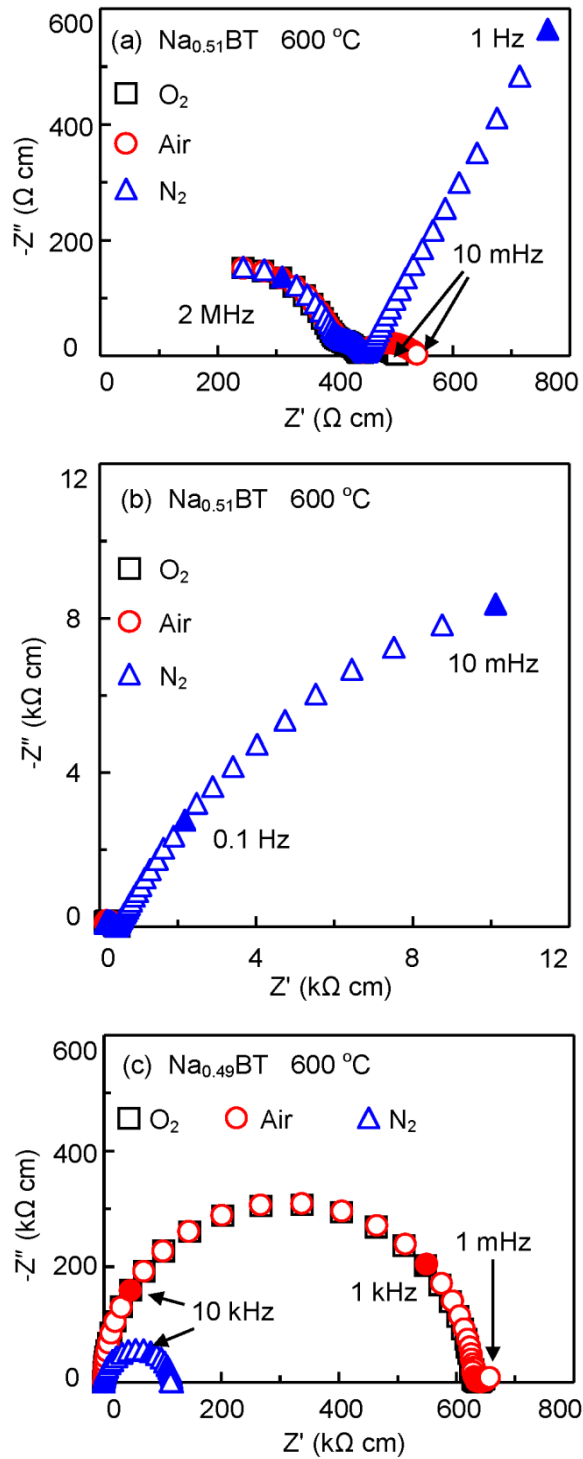
**Figure 3.** (a) Z* plots for $Na_{0.51}BT$ with Au electrodes under different atmospheres at 600 °C; (b) full-scale view showing the low frequency data for measurements in $N_2$; and (c) Z* plots for $Na_{0.49}T$ with Au electrodes at 600 °C under different atmospheres. Filled symbols indicate selected frequencies.

**[18]O tracer diffusion measurements**. The suppression of oxide-ion conduction is $Na_{0.49}BT$ was confirmed by [18]O tracer diffusion measurements using isotopic exchange and line scanning by secondary ion mass spectrometry (SIMS), Figure 4. At ~ 608 °C, the tracer diffusion coefficient (D*) is $3.2 \times 10^{-13}$ cm$^2$/s, surface exchange coefficient (k*) is $8.5 \times 10^{-9}$ cm/s. The tracer diffusion profile is < 2 μm and the D* value may be subjected to large error (50-100%). Nevertheless, D* is ca. three orders of magnitude lower than that of NBT at ~ 608 °C ($5.2 \times 10^{-13}$ cm$^2$/s, see Figure S5 in Supplementary Information in Ref. 30). The calculated oxide ion conductivity for $Na_{0.49}BT$ from D* using the Nernst-Einstein is ~ $1.4 \times 10^{-7}$ S cm$^{-1}$ at 608 °C, which is ca. one order of magnitude lower than the total conductivity ~$1.6 \times 10^{-6}$ S cm$^{-1}$ at 600 °C obtained from IS data, Figure 3c. This confirms the bulk conduction to be dominated by electronic species as opposed to oxide-ions.
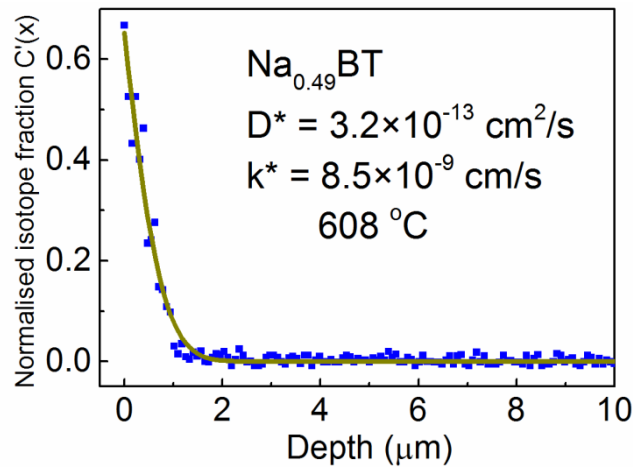


**Figure 4.** [18]O tracer diffusion profile for $Na_{0.49}BT$ after exchange at 608 °C for 8040 s with $p^{18}O_2$ ~ 750 mbar.
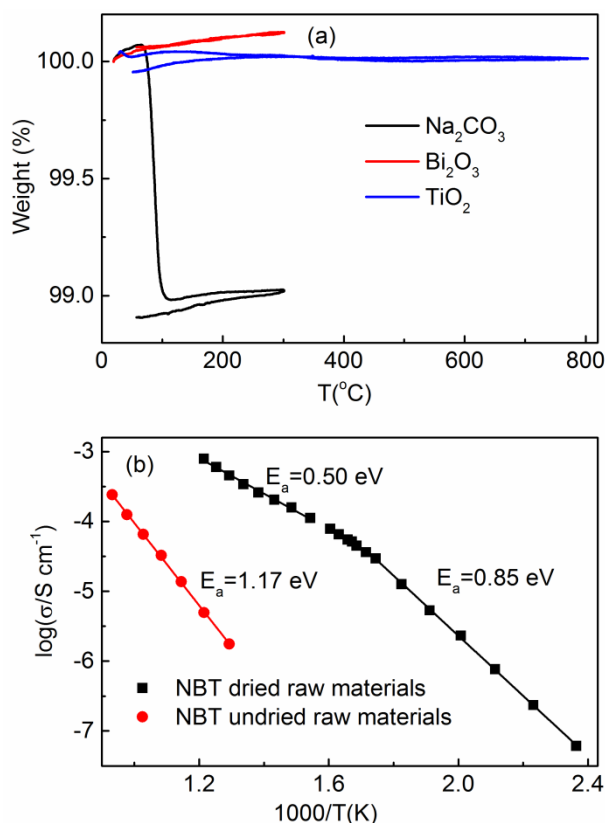
**Figure 5.** (a) TGA data of $Na_2CO_3$, $Bi_2O_3$ and $TiO_2$ reagents on a single heating and cooling cycle in air; (b) Arrhenius-type plots of bulk conductivity for wet- and dry-NBT samples.

**Influence of raw materials on electrical properties**. $Na_2CO_3$ is particularly hygroscopic and TGA data revealed an irreversible weight loss of ~ 1.0 wt% on heating in our reagent that we attribute to adsorbed water, Figure 5a. The precise water content will vary from batch to batch depending on how they are made and stored. In our case, the correct chemical formula for our undried $Na_2CO_3$ reagent can be considered as $Na_2CO_3.0.06H_2O$. Given the high sensitivity of the electrical properties of NBT on the starting Na and Bi contents, pre-treatment or drying of reagents may influence the starting stoichiometry and therefore the electrical properties obtained. In our studies, reagents are always dried at suitable temperatures prior to weighing to eliminate any adsorbed moisture and/or $CO_2$ to ensure the correct starting stoichiometry. Here we also prepared an additional sample (so-called wet-NBT) by using the three raw materials directly from the bottles without pre-drying but

assumed full stoichiometry for each reagent. As $Na_2CO_3$ reagent exhibits larger weight loss, this wet-NBT sample corresponds to a Na-deficient starting composition close to $Na_{0.495}Bi_{0.50}TiO_{2.9975}$ as opposed to $Na_{0.50}Bi_{0.50}TiO_3$ when using dried reagents (so-called dry-NBT). Arrhenius-type plots of bulk conductivity obtained from IS for two samples (wet- and dry-NBT) processed under identical conditions revealed the wet-NBT sample to display insulating behaviour with much lower $\sigma_b$ and a higher $E_a$ compared to the dry-NBT sample, Figure 5b.

## 4. Discussion

The results presented here for nominal Na-nonstoichiometric NBT combined with those obtained previously for nominal Bi-nonstoichiometric NBT[30] confirm non-stoichiometry to occur in this phase; however, it is rather difficult to quantify the level(s) and type(s) of non-stoichiometry based only on the nominal starting compositions. XRD results suggest phase-pure materials for all compositions studied but a combination of analytical SEM and TEM show only the nominal starting composition NBT to be phase-pure and therefore the A-site non-stoichiometry to be within $\pm$ 0.01 of the title compound $Na_{0.50}Bi_{0.50}TiO_3$, see Figure S2, Table S2 and Ref. 30 for more details. Unfortunately, common chemical techniques are incapable of detecting accurately such small compositional changes and distinguishing unambiguously these NBT samples with slightly different nominal compositions.

In the present study, small variations in the Na-starting content of NBT lead to significant changes in $\sigma_b$ and $E_a$, Figure 2. $Na_{0.51}BT$ exhibits $\sigma_b$ at least 4 orders or magnitude higher than $Na_{0.49}BT$ below 500 °C. The IS data obtained from measurements in air, Figure 2, and those obtained as a function of $pO_2$, Figure 3, show the higher $\sigma_b$ of $Na_{0.51}BT$ is associated with oxide-ion conduction, whereas in $Na_{0.49}BT$ the oxide-ion conductivity is suppressed. The $E_a$ for $Na_{0.49}BT$ is ~1.7 eV, Figure 2c. Based on the reported optical band gap ($E_g$) of

14

~3.0-3.5 eV for NBT,[34-36] the electrical conduction in $Na_{0.49}BT$ is close to/dominated by intrinsic electronic conduction (where $E_g \sim 2E_a$). The dominance of electronic conduction in the resistive composition $Na_{0.49}BT$ is confirmed by $^{18}O$ tracer diffusion measurements, Figure 4. The calculated oxide-ion conductivity from D* accounts for only ~ 10% of the total conductivity measured by IS.

The Arrhenius-type plots of $\sigma_b$, Figure 2c, show clearly there are two distinctive types of NBT compositions: one based on nominal Bi-deficiency (and/or $Bi_2O_3$ loss during processing of nominally stoichiometric NBT) that exhibit high oxide-ion conductivity; whereas, the other is close to stoichiometric NBT and is an excellent dielectric (dominated by intrinsic electronic conduction). It should be noted that Na nonstoichiometry influences electrical properties differently to Bi nonstoichiometry. The conducting Na-excess starting sample ($Na_{0.51}BT$) behaves similarly to the Bi-deficient starting sample ($NBi_{0.49}T$); whereas the resistive Na-deficient starting sample ($Na_{0.49}BT$) behaves similarly to Bi-excess starting sample ($NBi_{0.51}T$). In the series of Bi-varying compositions, $Na_{0.50}Bi_{0.50+x}TiO_{3+1.50x}$ where x = -0.01 ($Na_{0.50}Bi_{0.49}TiO_{2.985}$; $NBi_{0.49}T$) and 0.01 ($Na_{0.50}Bi_{0.51}TiO_{3.015}$; $NBi_{0.51}T$), it is straightforward to understand, based on equation (1), why the Bi-deficient composition is conducting and the Bi-excess composition is insulating. The apparent peculiar behaviour of nominal Na nonstoichiometric compositions, $Na_{0.50+y}Bi_{0.50}TiO_{3+0.50y}$ (y= 0.01 and -0.01) can be explained by the secondary phases revealed by SEM/TEM.

In the case of $Na_{0.49}BT$, the nominal starting composition is Na-deficient and, in principle, should be expected to generate oxygen vacancies. However, $TiO_2$ is observed as a secondary phase by TEM, suggesting a different final composition for the main NBT phase. The starting composition $Na_{0.49}BT$ can be renormalised to $Na_{0.50}Bi_{0.51}Ti_{1.02}O_{3.065}$ and can be considered as $Na_{0.50}Bi_{0.51}Ti_{1.02-z}O_{3.055-2z}$ + z $TiO_2$ (z $TiO_2$ represents the $TiO_2$ secondary phase). It is

therefore apparent that $Na_{0.49}BT$ is effectively a Bi-excess starting composition similar to $NBi_{0.51}T$ but with a different A/B site starting ratio, Table S2. The $Bi_2O_3$ loss induced during sample processing can be compensated by the excess $Bi_2O_3$ in the starting composition, resulting in suppressed oxygen vacancies and low levels of oxide-ion conductivity. This composition is therefore insulating with low dielectric loss and near-intrinsic electronic $\sigma_b$ up to ~ 600 °C, Figure 1b and 2c, respectively.

In the case of $Na_{0.51}BT$, SEM shows the presence of small amounts of a Na-rich secondary phase. The final composition after sintering is therefore effectively Bi-deficient due to $Bi_2O_3$ loss during sample processing, resulting in the formation of oxygen vacancies and oxide-ion conductivity. This composition is conducting above ~ 300 °C with high levels of dielectric loss and appreciable oxide-ion $\sigma_b$, Figure 1b and 2c, respectively.

The electrical properties of all nominal compositions with Na and Bi non-stoichiometry characterised to date are summarised in Table S2. Despite the low levels of A-site non-stoichiometry involved and the difficulties associated with suppressing loss of the A-site cations during processing (and in quantifying the final A-site composition of grains within sintered ceramics), we show unequivocally that NBT-based materials exhibit distinct electrical behaviour based on the nominal Bi/Na starting ratio. Ceramics from starting compositions with Bi/Na > 1 are electrically insulating with tan δ < 0.005 (at 300-600 °C), low $\sigma_b$ (with a large $E_a$ of ~ 1.7 eV) and D* for $^{18}O$ diffusion at 608 °C of ~ $10^{-13}$ cm$^2$/s and therefore suitable for piezoelectric/dielectric applications. In contrast, those prepared from Bi/Na ≤ 1 are predominantly oxide-ion conductors with high tan δ and high $\sigma_b$ (with $E_a$ < 1 eV) with D* for $^{18}O$ diffusion of ~ $10^{-10}$ cm$^2$/s at 608 °C that may be suitable as base compositions for the development of solid electrolytes/electrodes for intermediate/low temperatures solid oxide fuel cells. The switch in electrical conduction between electronic

and oxide ion conduction and the accompanied significant changes of electrical conductivity by low levels of A-site nonstoichiometry in undoped NBT is unique. Such a behaviour has not been observed in other known $(Ba,Sr,Ca)TiO_3$ perovskite oxides.

Perhaps the most striking demonstration of the sensitivity of NBT to exceptionally small compositional variations in the starting stoichiometry is the switch in $\sigma_b$ and conduction mechanism(s) observed for wet- and dry-NBT, Figure 5. The dry-NBT sample corresponds to a starting composition with Na/Bi = 1 and is therefore conducting due to $Bi_2O_3$ loss during processing. In contrast, the wet-NBT sample has a starting composition with Na/Bi < 1 and the excess $Bi_2O_3$ compensates for the $Bi_2O_3$ loss during ceramic processing and insulating properties are obtained. The level of adsorbed moisture in raw materials, especially $Na_2CO_3$ will vary from source to source. To obtain reproducible NBT-based materials for dielectric applications on a production scale, it is important the water content of raw materials is quantified to ensure sufficient adjustment of the Na/Bi starting ratio to obtain the desired insulating properties. Alternatively, raw materials should be pre-dried to eliminate the water content and a small excess of $Bi_2O_3$ added to the starting composition to ensure adequate compensation for any $Bi_2O_3$ loss associated with ceramic processing, based on equation (1). Failure to undertake either of these simple procedures to adjust the starting Na/Bi ratio could lead to significant changes in the properties of the final processed ceramics and is a likely explanation for the significant variation in high temperature dielectric properties of nominally undoped NBT ceramics reported in the literature.

It is unclear at this stage if a continuous solid solution exists between these two types of NBT or whether they are based on two, different but limited solid solutions. From the Arrhenius plots of $\sigma_b$ in Figure 2c, any solid solution based around dielectric NBT would appear to be extremely limited as $\sigma_b$ is essentially identical for two different starting compositions

($Na_{0.49}BT$ and $NBi_{0.51}T$), whereas there is a small but significant difference in $\sigma_b$ between the three conducting samples (NBT, $Na_{0.51}BT$ and $NBi_{0.49}T$) suggesting more variability in their compositions. Further studies are in progress to resolve this issue and to establish the solid solution range(s) in NBT.

Finally, it is worth commenting on the complex crystal structure of NBT reported in the literature.[18-25] Our work shows there are two types of NBT based on the level of non-stoichiometry (resistive stoichiometric NBT and conducting Bi-deficient NBT). It's not clear whether the NBT samples used in the structural studies reported in the literature are resistive or conducting and whether or not these two electrically distinct materials have the same crystal structure. This is worthy of further investigation.

## 5. Conclusions:

The electrical behaviour of NBT is highly sensitive to low levels of A-site nonstoichiometry. For the series of Na nonstoichiometric compositions, $Na_{0.50+y}Bi_{0.50}TiO_{3+0.50y}$ (y= 0.01 and -0.01), starting compositions with Na-excess exhibit higher $\sigma_b$ (by at least ~4 orders of magnitude below 500 °C) than the Na-deficient compositions due to the high oxide-ion conductivity in the former. Drying raw materials influences the starting stoichiometry slightly but can result in significant change in bulk conductivity and conduction mechanisms.

This work reveals two distinctive types of NBT compositions exist. One is close to stoichiometric NBT, exhibits near-intrinsic electronic conduction and is an excellent dielectric. Starting compositions with Bi/Na > 1 will lead to such insulating composition(s) which are suitable for dielectric/piezoelectric applications. The other type is Bi-deficient and exhibit high oxide-ion conductivity. Starting compositions with Bi/Na ≤ 1 will lead to such

conducting materials and these may be suitable (with appropriate doping) for fuel cell electrolyte/electrode applications.

**Supporting Information**

Data of XRD, SEM, TEM, EDS for characterisation of phase purity and ceramic microstructure. This material is available free of charge via the Internet at http://pubs.acs.org.
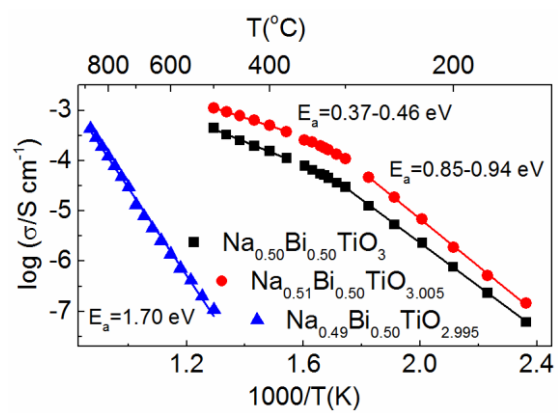
**References**

(1)      Y. Saito, H. Takao, T. Tani, T. Nonoyama, K. Takatori, T. Homma, T. Nagaya & M. Nakamura, Nature **2004**, 432, 84.

(2)      J. Rödel, W. Jo, K. T. P. Seifert, E. M. Anton, T. Granzow & D. Damjanovic, J. Am. Ceram. Soc. **2009**, 92, 1153.

(3)      M. D. Maeder, D. Damjanovic & N. Setter, J. Electroceram. **2004**, 13, 385.

(4)      T. Takenaka & H. Nagata, J. Eur. Ceram. Soc. **2005**, 25, 2693.

(5)      Y. Guo, Y. Liu, R. L. Withers, F. Brink & H. Chen, Chem. Mater. **2011**, 23, 219.

(6)      R. Dittmer, W. Jo, J. Roedel, S. Kalinin & N. Balke, Adv. Funct. Mater. **2012**, 22, 4208.

(7)      T. Takenaka, K.-i. Maruyama & K. Sakata, Jpn. J. Appl. Phys., Part 1 **1991**, 30, 2236.

(8)      B. J. Chu, D. R. Chen, G. R. Li & Q. R. Yin, J. Eur. Ceram. Soc. **2002**, 22, 2115.

(9)      X. X. Wang, X. G. Tang & H. L. W. Chan, Appl. Phys. Lett. **2004**, 85, 91.

(10)     S. T. Zhang, A. B. Kounga, E. Aulbach, T. Granzow, W. Jo, H. J. Kleebe & J. Rödel, J. Appl. Phys. **2008**, 103, 034107.

(11)     W. Jo, T. Granzow, E. Aulbach, J. Rödel & D. Damjanovic, J. Appl. Phys. **2009**, 105, 094102.

(12)     Y. Hiruma, H. Nagata & T. Takenaka, J. Appl. Phys. **2008**, 104, 124106.

(13)  J. Zang, W. Jo, H. Zhang & J. Rödel, J. Eur. Ceram. Soc. **2014**, 34, 43.

(14)  E. A. Patterson, D. P. Cann, J. Pokorny & I. M. Reaney, J. Appl. Phys. **2012**, 111, 094105.

(15)  R. Dittmer, E.-M. Anton, W. Jo, H. Simons, J. E. Daniels, M. Hoffman, J. Pokorny, I. M. Reaney & J. Rödel, J. Am. Ceram. Soc. **2012**, 95, 3519.

(16)  Y. M. Chiang, G. W. Farrey & A. N. Soukhojak, Appl. Phys. Lett. **1998**, 73, 3683.

(17)  H. Yilmaz, G. L. Messing & S. Trolier-McKinstry, J. Electroceram. **2003**, 11, 207.

(18)  G. O. Jones & P. A. Thomas, Acta Crystallogr., Sect. B: Struct. Sci **2002**, 58, 168.

(19)  E. Aksel, J. S. Forrester, J. L. Jones, P. A. Thomas, K. Page & M. R. Suchomel, Appl. Phys. Lett. **2011**, 98, 152901.

(20)  D. S. Keeble, E. R. Barney, D. A. Keen, M. G. Tucker, J. Kreisel & P. A. Thomas, Adv. Funct. Mater. **2012**, 23, 185.

(21)  E. Aksel, J. S. Forrester, J. C. Nino, K. Page, D. P. Shoemaker & J. L. Jones, Phys. Rev. B **2013**, 87, 104113.

(22)  I. Levin & I. M. Reaney, Adv. Funct. Mater. **2012**, 22, 3445.

(23)  V. Dorcet, G. Trolliard & P. Boullay, Chem. Mater. **2008**, 20, 5061.

(24)  G. Trolliard & V. Dorcet, Chem. Mater. **2008**, 20, 5074.

(25)  M. Groeting, S. Hayn & K. Albe, J. Solid State Chem. **2011**, 184, 2041.

(26)  Y. Hiruma, H. Nagata & T. Takenaka, J. Appl. Phys. **2009**, 105, 084112.

(27)  Y. S. Sung, J. M. Kim, J. H. Cho, T. K. Song, M. H. Kim, H. H. Chong, T. G. Park, D. Do & S. S. Kim, Appl. Phys. Lett. **2010**, 96, 022901.

(28)  Y. S. Sung, J. M. Kim, J. H. Cho, T. K. Song, M. H. Kim & T. G. Park, Appl. Phys. Lett. **2011**, 98, 012902.

(29)  M. Spreitzer, M. Valant & D. Suvorov, J. Mater. Chem. **2007**, 17, 185.

(30)    M. Li, M. J. Pietrowski, R. A. De Souza, H. Zhang, I. M. Reaney, S. N. Cook, J. A. Kilner & D. C. Sinclair, Nat. Mater. **2014**, 13, 31.

(31)    D. Schütz, M. Deluca, W. Krauss, A. Feteira, T. Jackson & K. Reichmann, Adv. Funct. Mater. **2012**, 22, 2285.

(32)    R. A. De Souza & M. Martin, MRS Bull. **2009**, 34, 907.

(33)    J. A. Kilner, S. J. Skinner & H. H. Brongersma, J. Solid State Electrochem. **2011**, 15, 861.

(34)    M. Bousquet, J. R. Duclere, E. Orhan, A. Boulle, C. Bachelet & C. Champeaux, J. Appl. Phys. **2010**, 107, 104107.

(35)    C. Y. Kim, T. Sekino & K. Niihara, J. Sol-Gel Sci. Technol. **2010**, 55, 306.

(36)    M. Zeng, S. W. Or & H. L. W. Chan, J. Appl. Phys. **2010**, 107, 043513.

**Table of Contents/Abstract Graphic**

**The dramatic influence of A-site non-stoichiometry on the electrical conductivity and conduction mechanisms in the perovskite oxide Na$_{0.5}$Bi$_{0.5}$TiO$_3$**

Ming Li[1], Huairuo Zhang[1], Stuart N. Cook[2], Linhao Li[1], John A. Kilner[2,3], Ian M. Reaney[1] and Derek C. Sinclair[1*]

[1]Department of Materials Science and Engineering, University of Sheffield, Sir Robert Hadfield Building, Mappin Street, Sheffield, S1 3JD, United Kingdom.

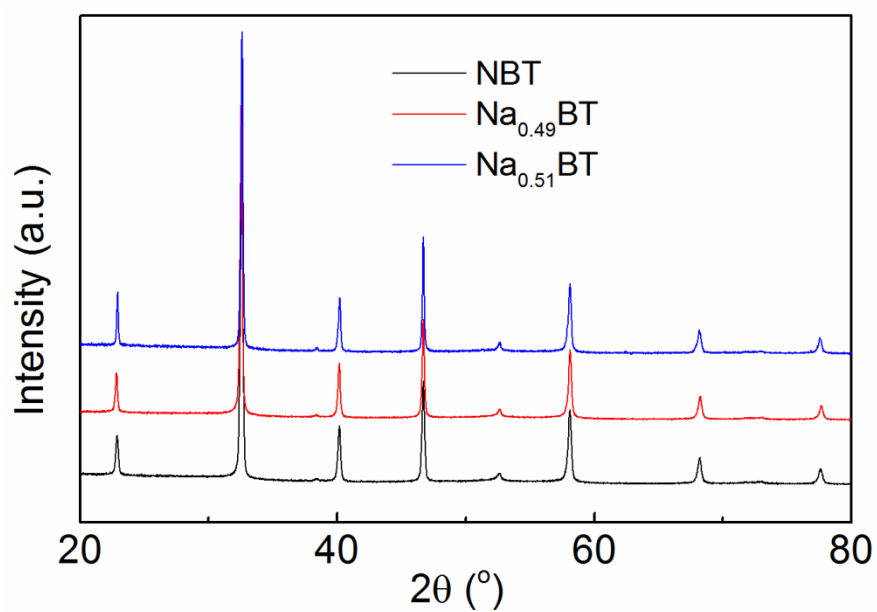[2]Department of Materials, Imperial College London, London, SW7 2AZ, United Kingdom.

[3]International Institute for Carbon-Neutral Energy Research (I2CNER), 744 Motooka Nishi-ku Fukuoka 819-0395, Japan.

* Author to whom correspondence should be addressed.
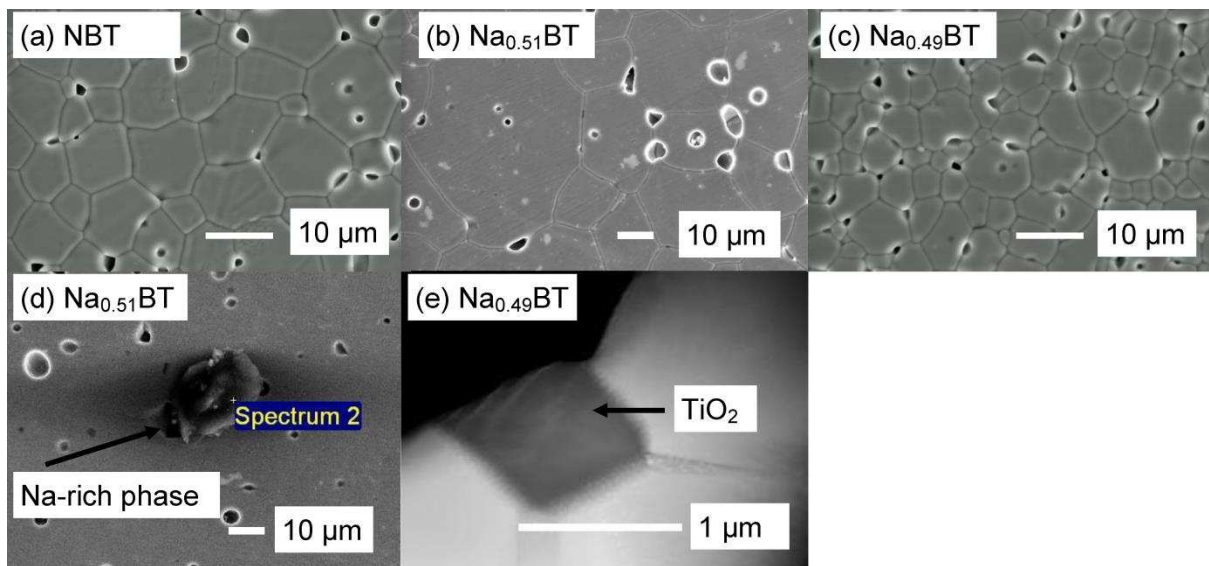
E-mail: d.c.sinclair@sheffield.ac.uk.

**XRD**



**Figure S1.** XRD patterns of NBT (bottom), $Na_{0.49}BT$ (middle) and $Na_{0.51}BT$ (top) after double calcination at 800 and 850 °C for 2h.

**SEM/TEM**



**Figure S2.** top panel: SEM micrographs of a) NBT, b) $Na_{0.51}BT$ and c) $Na_{0.49}BT$. All samples were polished and thermally etched prior to SEM. Bottom panel: d) secondary electron image of an $Na_{0.51}BT$ ceramic (polished without thermal etching) showing the Na-rich secondary phase, and e) a STEM high angle annular dark field (HAADF) Z-contrast image showing the $TiO_2$ secondary phase in $Na_{0.49}BT$.

**Table S1.** Local and average compositions by EDS. Data were obtained by measurements on at least 10 randomly selected areas. The mean value and standard deviation are listed.

|  | Na (at%) | Bi (at%) | Ti (at%) |
|---|---|---|---|
| $Na_{0.51}BT$ | 25.09 ($\pm$0.48) | 25.14 ($\pm$0.34) | 49.77 ($\pm$0.32) |
| NBT | 25.03 ($\pm$0.43) | 25.17 ($\pm$0.21) | 49.80 ($\pm$0.36) |
| $Na_{0.49}BT$ | 24.72 ($\pm$0.57) | 25.36 ($\pm$0.22) | 49.92 ($\pm$0.54) |

**Table S2.** Summary of various compositions (including A-/B-site and Bi/Na ratios), their electrical behaviour and additional phases observed by SEM or TEM. See Ref. 30 for more details on Bi-rich and Bi-deficient starting compositions.

| Composition | A/B | Bi/Na | Conducting/Insulating | Extra phases |
|---|---|---|---|---|
| $Na_{0.50}Bi_{0.50}TiO_3$ | 1 | 1 | Conducting | Phase pure |
| $Na_{0.50}Bi_{0.51}TiO_{3.015}$ (A-site excess and Bi-rich) | 1.01 | 1.02 | Insulating | $Bi_2O_3$ [Ref. 30] (TEM) |
| $Na_{0.50}Bi_{0.49}TiO_{2.985}$ (A-site and Bi-deficient) | 0.99 | 0.98 | Conducting | $Na_2Ti_6O_{13}$ [Ref. 30] (SEM) |
| $Na_{0.51}Bi_{0.50}TiO_{3.005}$ (A-site excess and Na-rich) | 1.01 | 0.98 | Conducting | Na-rich (SEM) |
| $Na_{0.49}Bi_{0.50}TiO_{2.995}$ (A-site and Na-deficient) | 0.99 | 1.02 | Insulating | $TiO_2$ (TEM) |